

## Photovoltaic Power Conversion System Based on Cascaded Inverters with Synchronized Space-Vector Modulation

V. Oleschuk<sup>1</sup>, J. Tlustý<sup>2</sup> and V. Valouch<sup>3</sup>

<sup>1</sup> Institute of Power Engineering of the Academy of Sc., Kishinau, Moldova, and Politecnico di Torino, Turin, 10129, Italy  
Phone: +039 011 0907111, Fax: +039 011 0907111, E-mail: oleschukv@hotmail.com

<sup>2</sup> Department of Power Engineering, Faculty of Electrical Engineering, CTU, Prague, Czech Republic  
E-mail: tlusty@fel.cvut.cz

<sup>3</sup> Institute of Thermomechanics of the Academy of Sc. of Czech Republic, Dolejskova 5, Prague, Czech Republic  
E-mail: valouch@it.cas.cz

**Abstract.** The paper presents results of investigation of dual-inverter-based power conversion system with synchronized pulsewidth modulation (PWM) for photovoltaic application. This system topology includes two insulated strings of photovoltaic panels, feeding two standard three-phase inverters, connected to grid by a three-phase transformer with the open winding configuration on primary side. Algorithms of synchronized PWM provide in this case continuous voltage synchronization both in each inverter and in the load. Simulations show a behavior of the systems with low switching frequency, with both continuous and discontinuous versions of synchronized PWM.

### Key words

Cascaded two-level inverters, photovoltaic application, modulation strategy, voltage synchronization.

### 1. Introduction

Multilevel converters and drives are a subject of increasing interest in the last years due to some advantages compared with conventional three-phase systems. Some of the perspective topologies of power converters are now cascaded (dual) two-level converters which utilize two standard three-phase voltage source inverters [1]-[3]. In particular, dual inverter-fed open-end winding motor drives have some advantages such as redundancy of the space-vector combinations and the absence of neutral point fluctuations [4]-[7]. These new drive topologies provide also one of the best possible use of semiconductor switches.

Almost all versions of classical space-vector PWM are based on the asynchronous principle, which results in sub-harmonics (of the fundamental frequency) in the spectrum of the output voltage of converters, which are

very undesirable in medium/high power applications [8]-[9]. In order to provide voltage synchronization in dual inverter-fed drives, a novel method of synchronized PWM has been applied for control of these systems with single dc voltage source [10], and for the systems with two dc sources: without power balancing between sources [11], and also with power balancing PWM algorithms in a linear control range [12].

Besides adjustable speed ac drives, photovoltaic systems are between perspective areas of application of the dual-inverter topology [13]. In particular, Fig. 1 presents dual inverter system supplied by two insulated strings of photovoltaic panels with the resulting dc voltages  $V_L$  and  $V_H$  [13]. Direct connection of photovoltaic modules to inverters, or their connection through dc/dc link (dashed lines in Fig. 1) is available in this case. Dual inverters are connected to grid by a three-phase transformer with the open winding configuration on primary side.

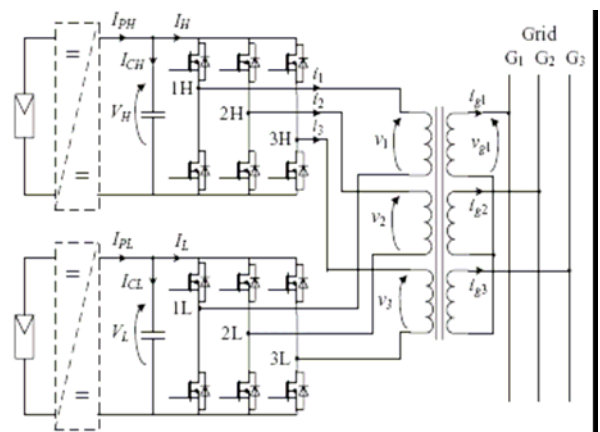


Fig. 1. Topology of cascaded-inverter-based photovoltaic system [13].

The presented configuration of power circuits is one of the most suitable for photovoltaic systems with a higher power range. So, this paper presents results of dissemination of novel method of synchronized pulsewidth modulation for control of cascaded-inverter-based power conversion system for photovoltaic high power/high current application.

## 2. Features of the Method of Synchronized PWM

In order to avoid asynchronous operation of inverters with conventional space-vector modulation, novel space-vector-based method of synchronized PWM [14],[15] can be used for control of each inverter in a dual system for photovoltaic application.

Figs. 2 - 3 present switching state sequences of standard three-phase inverter inside the interval  $0^0-90^0$ . It illustrates schematically basic continuous (Fig. 2) and discontinuous (Fig. 3) versions of space-vector PWM.

The upper traces in Figs. 2 – 3 are switching state sequences (in accordance with conventional designation [14]), then – control signals for the cathode switches of the corresponding phases of each inverter. The lower traces in Figs. 2 - 3 show the corresponding quarter-wave of the line output voltage of inverter. Signals  $\beta_j$  represent total switch-on durations during switching sub-intervals  $\tau$ , signals  $\gamma_k$  are generated on the borders (Fig. 2) or in the centers (Fig. 3) of the corresponding  $\beta$ . Widths of notches  $\lambda_k$  represent the duration of zero sequences [14].

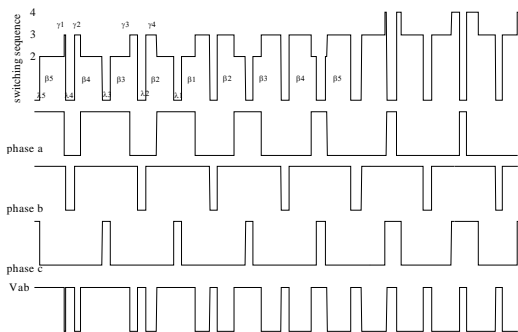


Fig. 2. Control and output signals of inverter with continuous PWM.

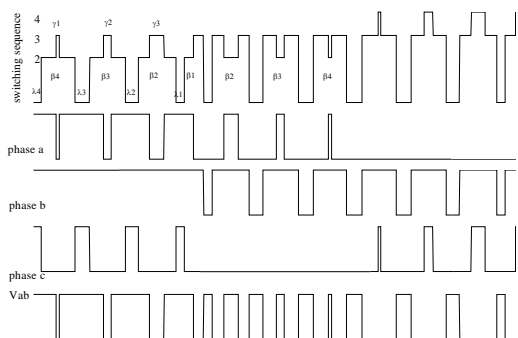


Fig.3. Control and output signals of inverter with discontinuous PWM.

So, one of the basic ideas of the proposed PWM method is in continuous synchronization of the positions of all central signals  $\beta_1$  in the centers of the  $60^0$  clock-intervals (to fix positions of  $\beta_1$  in the centers of the cycles), and then – to generate symmetrically all other active  $\beta$  - and  $\gamma$  -signals, together with the corresponding notches.

Determination of parameters of basic control signals of synchronized space-vector scheme of PWM for each inverter of dual inverter system can be described by (1)-(4) [14]:

For  $j=2, \dots, i$ :

$$\beta_1 = 1.1m\tau \quad (1)$$

$$\beta_j = \beta_1 \cos[(j-1)\tau] \quad (2)$$

$$\gamma_j = \beta_{i-j+1} \{0.5 - 0.866 \tan[(i-j)\tau]\} \quad (3)$$

$$\lambda_j = \tau - (\beta_j + \beta_{j+1})/2 \quad (4)$$

## 3. Synchronous Operation of Dual Inverters

Synchronous control of the output voltage of each inverter of dual-inverter system with synchronized PWM provides synchronous symmetrical regulation of the phase voltages  $V_1$ ,  $V_2$  and  $V_3$  of the system. Rational phase shift between output voltage waveforms of the two inverters is equal in this case to one half of the switching interval (sub-cycle)  $\tau$  [1].

In the case, when the two dc-link voltage sources have equal voltages ( $V_L=V_H$ ), the resulting voltage space-vectors are equal to the space-vector patterns of conventional three-level inverter [1],[3],[7].

The phase voltages  $V_1$ ,  $V_2$ ,  $V_3$  of the dual-inverter system with two insulated DC-link sources (Fig. 1) are calculated in accordance with (5)-(8) [4]:

$$V_0 = 1/3(V_{1L} + V_{2L} + V_{3L} + V_{1H} + V_{2H} + V_{3H}) \quad (5)$$

$$V_1 = V_{1L} + V_{1H} - V_0 \quad (6)$$

$$V_2 = V_{2L} + V_{2H} - V_0 \quad (7)$$

$$V_3 = V_{3L} + V_{3H} - V_0, \quad (8)$$

where  $V_{1L}$ ,  $V_{2L}$ ,  $V_{3L}$ ,  $V_{1H}$ ,  $V_{2H}$ ,  $V_{3H}$  are the pole voltages of each three-phase inverter (Fig. 1),  $V_0$  is the zero sequence (triplen harmonic components) voltage.

Control of photovoltaic power conversion systems on the base of dual inverters has some peculiarities. In the case of direct connection between the two photovoltaic strings and the two inverters, in order to provide maximum power point tracking of photovoltaic panels, control of the system should be based on the corresponding specific

regulation of modulation indices of dual inverters [13]. And this control is somewhat similar to power sharing process between two dual inverters for traction systems, analyzed in [7],[12].

Also, the fundamental frequency of the phase voltages of dual inverters should be equal to the fundamental frequency of the grid. In the case of fluctuation of the grid frequency the inverters' fundamental frequency should be correlated correspondingly. And control of two inverters in dual-inverter system can be often based on undermodulation control algorithms for one inverter, and on overmodulation PWM scheme for other inverter.

For photovoltaic power conversion system (Fig. 1) with close to constant fundamental frequency rational determination of the average switching frequency  $F_s$  of inverters and duration of sub-cycles  $\tau$  in function of the fundamental frequency  $F$  for continuous (CPWM) and discontinuous (DPWM) versions of PWM can be based on (9)-(11) [15]:

$$F_{s(CPWM)} = F(6n - 3) \quad (9)$$

$$F_{s(DPWM)} = F(8n - 5) \quad (10)$$

$$\tau = 1/2F_s, \quad (11)$$

where  $n=2,3,4,\dots$

In order to provide maximum power point tracking of photovoltaic panels and stabilization of the magnitude of the fundamental harmonic of the phase voltage of a dual-inverter system for photovoltaic application, the corresponding control system has been proposed, described and verified [13]. In particular, in the case of low dc-links voltages (it corresponds to low solar irradiation) modulation indices  $m_H$  and  $m_L$  of two inverters should be high, and the phase voltage has three-level waveform. In the case of higher dc-link voltages (this control mode corresponds to higher level of solar irradiation), modulation indices of the two modulated inverters should be decreased correspondingly, in order to provide close to constant amplitude of the phase voltage during solar irradiation fluctuations.

As an example of operation of the dual-inverter system with synchronized PWM under two control modes with different dc voltages, Fig. 4 – Fig. 7 present basic voltage waveforms (period of the pole voltages  $V_{IH}$ ,  $V_{IL}$ , line-to-line voltages  $V_{IH2H}$ ,  $V_{IL2L}$  of the two inverters, and phase voltage  $V_I$  (with its spectrum)) for the system with high (Figs. 4 and 5) and low (Figs. 6 and 7) dc-links voltages. Fundamental frequency of the system  $F=50\text{Hz}$ , and average switching frequency  $F_s=1.35\text{kHz}$  for each inverter. Figs. 4 and 6 show basic voltage waveforms of the system with continuous synchronized PWM, supplied by high (Fig. 4,  $m_H=m_L=0.45$ ) and low (Fig. 6,  $m_H=m_L=0.9$ ) dc-links voltages, which magnitude ratio is 2:1. Figs. 5 and 7 present the corresponding voltage waveforms (with spectra of the  $V_I$  voltage) for the system with discontinuous synchronized PWM.

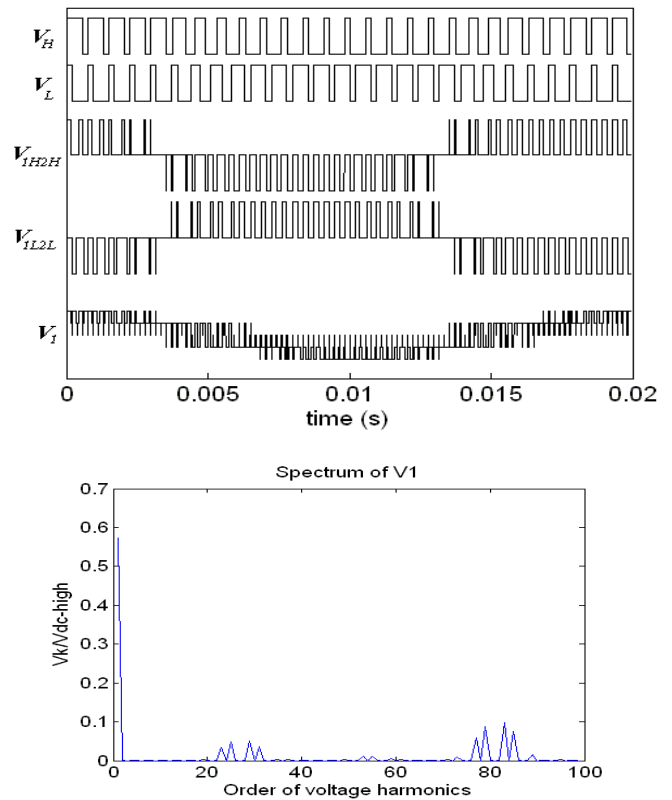


Fig. 4. Pole voltages  $V_{IH}$  and  $V_{IL}$ , line voltages  $V_{IH2H}$  and  $V_{IL2L}$ , and phase voltage  $V_I$  (with its spectrum) for the system with continuous synchronized PWM ( $F=50\text{Hz}$ ,  $F_s=1.35\text{kHz}$ ,  $V_H=V_L$ ,  $m_H=m_L=0.45$ ).

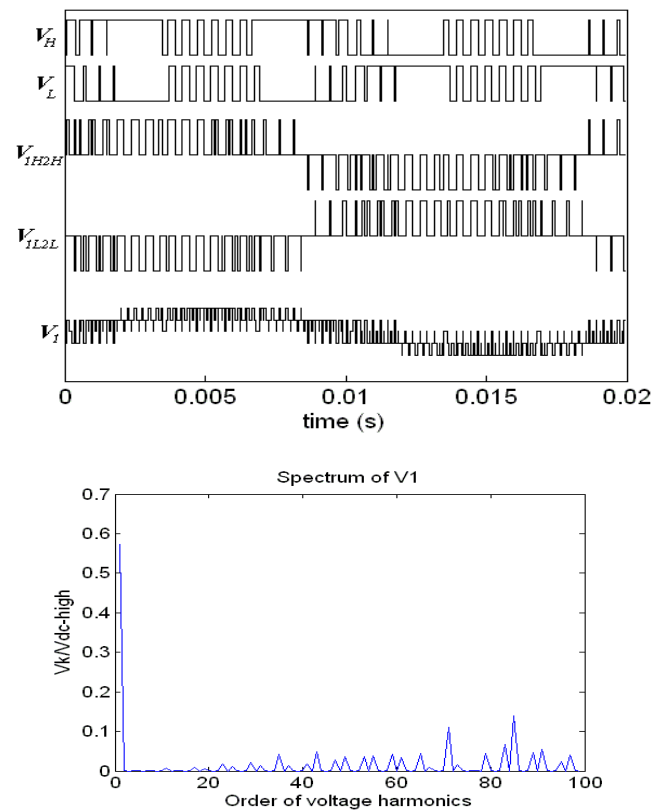


Fig. 5. Pole voltages  $V_{IH}$  and  $V_{IL}$ , line voltages  $V_{IH2H}$  and  $V_{IL2L}$ , and phase voltage  $V_I$  (with its spectrum) for the system with discontinuous synchronized PWM ( $F=50\text{Hz}$ ,  $F_s=1.35\text{kHz}$ ,  $V_H=V_L$ ,  $m_H=m_L=0.45$ ).

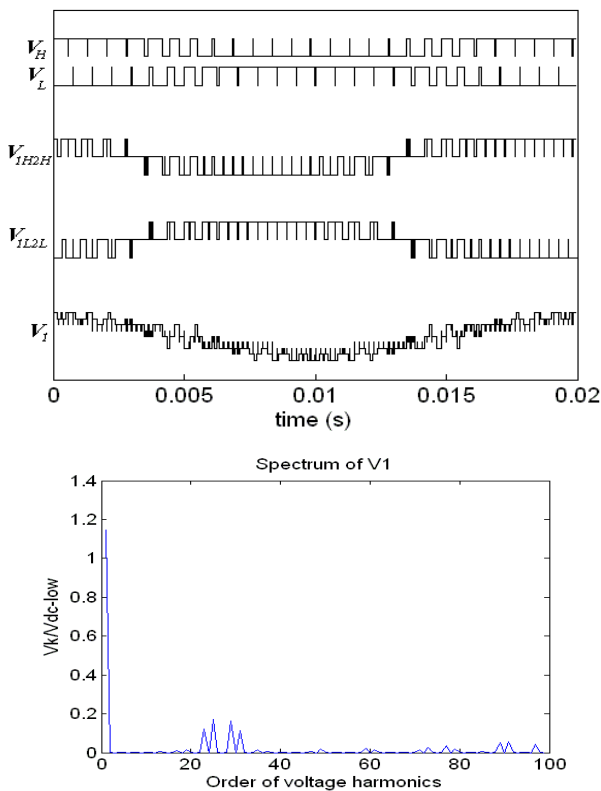


Fig. 6. Pole voltages  $V_{IH}$  and  $V_{IL}$ , line voltages  $V_{IH2H}$  and  $V_{IL2L}$ , and phase voltage  $V_I$  (with its spectrum) for the system with continuous synchronized PWM ( $F=50\text{Hz}$ ,  $F_s=1.35\text{kHz}$ ,  $V_H=V_L$ ,  $m_H=m_L=0.9$ ).

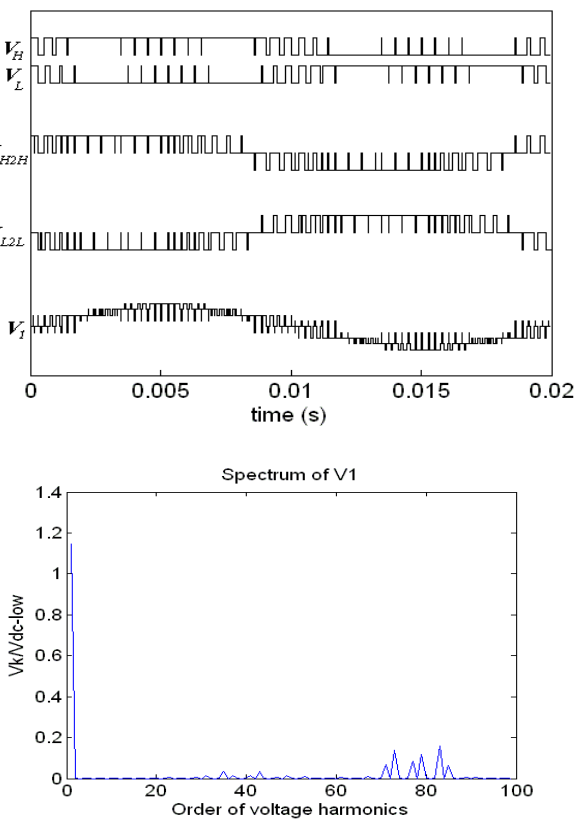


Fig. 7. Pole voltages  $V_{IH}$  and  $V_{IL}$ , line voltages  $V_{IH2H}$  and  $V_{IL2L}$ , and phase voltage  $V_I$  (with its spectrum) for the system with discontinuous synchronized PWM ( $F=50\text{Hz}$ ,  $F_s=1.35\text{kHz}$ ,  $V_H=V_L$ ,  $m_H=m_L=0.9$ ).

Fig. 8 and Fig. 9 present basic voltage waveforms (with spectrum of the  $V_I$  voltage) for the systems with different dc-links voltages ( $V_H=0.5V_L$ , and this fact can be connected with different level of solar irradiation for the two strings of photovoltaic panels). Diagrams in Fig. 8 correspond to the power conversion system controlled by algorithms of continuous synchronized PWM. Diagrams in Fig. 9 illustrate processes in the system with discontinuous synchronized modulation. Modulation indices of the two inverters of the systems should be different in this case, in particular,  $m_H=0.9$  and  $m_L=0.45$ .

Analysis of spectral characteristics of the phase voltage of the cascaded-inverter system shows (see Figs. 4 - 9), that algorithms of synchronized PWM provide symmetry of the phase voltage, and its spectra do not contain even harmonics and sub-harmonics for any control regime of the system, with both equal and different voltages of the two dc-sources.

Fig. 10 presents the calculation results of Total Harmonic Distortion factor ( $THD$ ) in the function of modulation indices  $m=m_H=m_L$  for the phase voltage  $V_I$  ( $THD = (1/V_1) \sqrt{\sum_{k=2}^{1000} (V_{1k})^2}$ ) of dual-inverter system

with equal dc-links voltages ( $V_H=V_L$ ), controlled by algorithms of continuous (CPWM) and discontinuous (DPWM) schemes of synchronized modulation. The fundamental frequency of the system is  $50\text{Hz}$ , and the average switching frequency for each modulated inverter is  $1.35\text{kHz}$ .

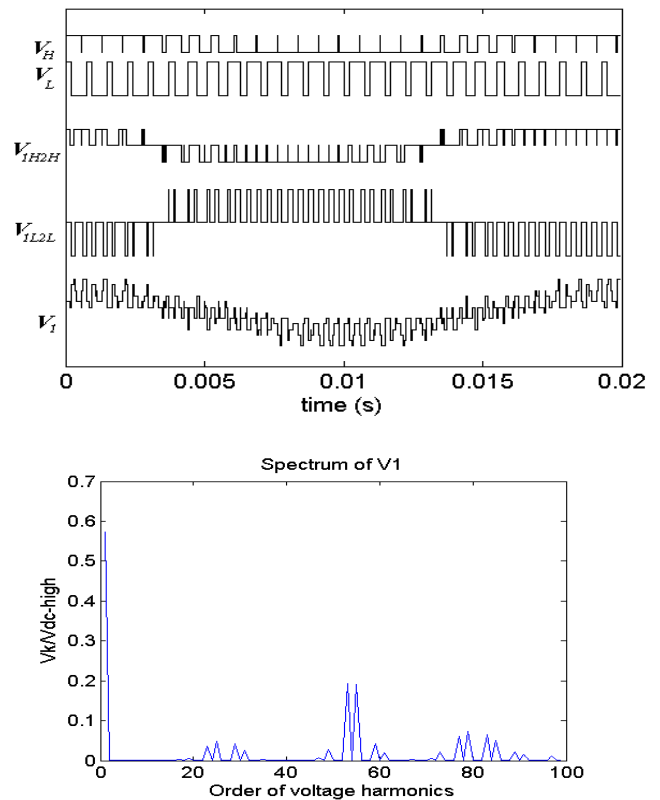


Fig. 8. Pole voltages  $V_{IH}$  and  $V_{IL}$ , line voltages  $V_{IH2H}$  and  $V_{IL2L}$ , and phase voltage  $V_I$  (with its spectrum) for the system with continuous synchronized PWM ( $F=50\text{Hz}$ ,  $F_s=1.35\text{kHz}$ ,  $V_H=0.5V_L$ ,  $m_H=0.9$ ,  $m_L=0.45$ ).

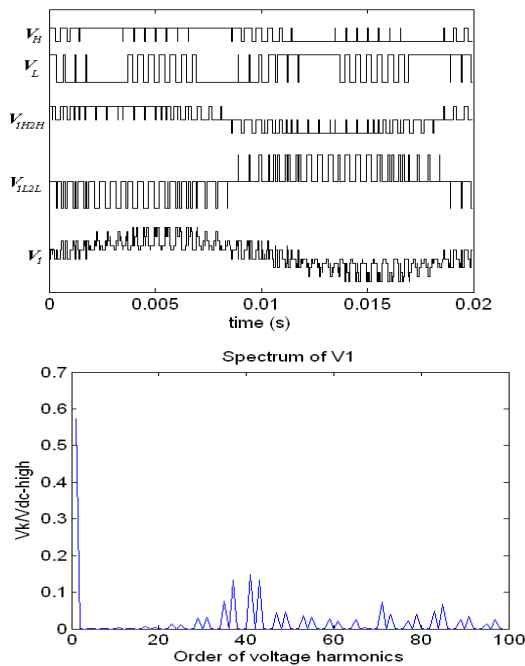


Fig. 9. Pole voltages  $V_{IH}$  and  $V_{IL}$ , line voltages  $V_{IH2H}$  and  $V_{IL2L}$ , and phase voltage  $V_I$  (with its spectrum) for the system with discontinuous synchronized PWM ( $F=50\text{Hz}$ ,  $F_s=1.35\text{kHz}$ ,  $V_H=0.5V_L$ ,  $m_H=0.9$ ,  $m_L=0.45$ ).

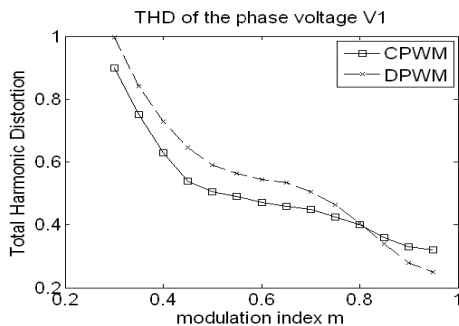


Fig. 10. THD factor of the phase voltage  $V_I$  versus modulation index  $m=m_H=m_L$ .

The calculation results presented in Fig. 10 show that continuous scheme of synchronized PWM provides better spectral composition of phase voltage in the systems with modulation indices  $m < 0.8$ , and discontinuous version of synchronized PWM provides better phase voltage spectra in dual-inverter systems operating under higher values of modulation index.

#### 4. Conclusion

Novel method of synchronized space-vector modulation, applied for control of dual-inverter system with two insulated photovoltaic dc-links, allows both continuous phase voltage synchronization and required regulation of the system by the corresponding control of modulation indices of two inverters.

The spectra of the phase voltage of the systems with algorithms of synchronized PWM do not contain even harmonics and sub-harmonics for any control regime of the systems, with both equal and different voltages of two

dc-sources, which is especially important for high power/high current applications.

Analysis of spectral composition of the phase voltage in dual-inverter photovoltaic power conversion systems shows advantage of the using of continuous scheme of synchronized PWM (in comparison with the scheme of discontinuous synchronized modulation) for the systems, operating under modulation indices  $0.8 > m > 0$ .

#### Acknowledgement

The financial supports of the Grant Agency of the Academy of Sciences of the Czech Republic (project No. IAA200760703), Institutional Research Plan Z20570509 of the Institute of Thermomechanics of the ASCR, v.v.i., and of the Ministry of Education, Youth and Sports (Research Plan MSM 6840770017 of the Czech Technical University) are highly acknowledged.

#### References

- [1] H. Stemmler and P. Guggenbach, "Configurations of high power voltage source inverter drives," EPE'93, pp. 7-12.
- [2] H. Stemmler, "High-power industrial drives," IEEE Proc., vol. 82, pp. 1266-1286, 1994.
- [3] K.A. Corzine, S.D. Sudhoff and C.A. Whitcomb, "Performance characteristics of a cascaded two-level converter," IEEE Trans. EC, vol. 14, pp. 433-439, 1999.
- [4] E.G. Shivakumar, K. Gopakumar, S.K. Sinha, A. Pittet and V.T. Ranganathan, "Space vector PWM control of dual inverter fed open-end winding induction motor drive," in Proc. APEC'2001, pp. 399-405.
- [5] E.G. Shivakumar, V.T. Somasekhar, K.K. Mohapatra, K. Gopakumar, L. Umanand and S.K. Sinha, "A multi level space phasor based PWM strategy for an open-end winding induction motor drive using two inverters with different dc-link voltages," in Proc. PEDS'2001, pp. 169-175.
- [6] M.R. Baiju, K.A. Mohapatra, R.S. Kanchan and K. Gopakumar, "A dual two-level inverter scheme with common mode voltage elimination for an induction motor drive," IEEE Trans. P EL, vol. 19, pp. 794-805, 2004.
- [7] G. Grandi, C. Rossi, A. Lega and D. Casadei, "Multilevel operation of a dual two-level inverter with power balancing capability," in CD-ROM Proc. IAS'2006, 8 p.
- [8] J. Holtz, "Pulsewidth modulation - a survey," IEEE Trans. Ind. Electr., vol. 39, pp. 410-420, 1992.
- [9] N. Mohan, T.M. Undeland and W.P. Robbins, Power Electronics, 3<sup>rd</sup> ed., John Wiley & Sons, 2003.
- [10] V. Oleschuk, F. Profumo, G. Griva, R. Bojoi and A.M. Stankovic, "Analysis and comparison of basic schemes of synchronized PWM for dual inverter-fed drives," in Proc. ISIE'2006, pp. 2455-2461.
- [11] V. Oleschuk, A. Sizov, F. Profumo, A. Tenconi and A.M. Stankovic, "Multilevel dual inverter-fed drives with synchronized PWM," in CD-ROM Proc. PESC'2006, 7 p.
- [12] V. Oleschuk, R. Bojoi, G. Griva and F. Profumo, "Dual inverter-fed traction drives with dc sources power balancing based on synchronized PWM", in Proc. IEMDC'2007, pp. 260-265.
- [13] G. Grandi, D. Ostojic, C. Rossi and A. Lega, "Control strategy for a multilevel inverter in grid-connected photovoltaic applications," in CD-ROM Proc. 2007 Aegean Conf. on Electrical Machine, Power Electron. and Electromotion, 6 p.
- [14] V. Oleschuk and F. Blaabjerg, "Direct synchronized PWM techniques with linear control functions for adjustable speed drives," in Proc. APEC'2002, pp. 76-82.
- [15] V. Oleschuk and F. Blaabjerg, "Quasi-linear algorithms of synchronous PWM for speed controlled induction motor drives," in CD-ROM Proc. ICEM'2002, 6 p.